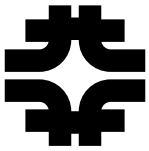

Fermi National Accelerator Laboratory

FERMILAB-Pub-96/037

A Detailed Calibration of a Stack Monitor Used in the Measurement of Airborne Radionuclides at a High Energy Proton Accelerator

Kamran Vaziri et al.

Fermi National Accelerator Laboratory
P.O. Box 500, Batavia, Illinois 60510

February 1996

Submitted to *Health Physics*

Operated by Universities Research Association Inc. under Contract No. DE-AC02-76CHO3000 with the United States Department of Energy

Disclaimer

A DETAILED CALIBRATION OF A STACK MONITOR USED IN THE MEASUREMENT OF AIRBORNE RADIONUCLIDES AT A HIGH ENERGY PROTON ACCELERATOR

Kamran Vaziri, Vernon R. Cupps, J. Donald Cossairt, David J. Boehnlein, and Alexander J. Elwyn

Fermi National Accelerator Laboratory

P.O. Box 500

Batavia, IL 60510

ABSTRACT

A method for calibrating a stack monitor used to continuously monitor airborne radionuclide emissions at a high energy proton accelerator was developed from basic principles involving the relevant physical effects. The methods of calculating the absolute efficiency are presented in detail. These methods have general application and are suitable for employment at similar installations irrespective of energy or particle type being accelerated. Results are presented for a particular measurement as an example of the applicability and validity of the technique[#].

INTRODUCTION

In order to assure compliance with governmental regulations designed to provide protection against ionizing radiation for the environment and the general public, it is necessary to identify and measure the airborne radionuclides released due to the operation of particle accelerators. In the United States, the United States Environmental Protection Agency has promulgated regulations which imposed an annual limit to the dose equivalent that can be delivered to an individual member of the public by means of this pathway as a result of the operations of United States Department of Energy Facilities. This limit is 10^{-4} Sv (10 mrem) (U. S. Environmental Protection Agency, 1989). Given this relatively low annual limit of dose equivalent, especially if the dose equivalent is delivered approximately uniformly in time, it is necessary to monitor significant sources of radionuclides due to accelerator operations on a continuous basis with considerable accuracy. The emphasis in this paper is on a method of calibration of a stack monitor and a description of results obtained in the process of performing the calibration.

The production of airborne radionuclides at particle accelerators is perhaps best summarized in the seminal work of Patterson and Thomas (1973). More recent general references on this topic are those of Thomas and Stevenson (1988) and Swanson and Thomas (1990). As presented in these references, the collective experience of the world-wide accelerator radiation protection community is that the positron-emitting radionuclides ^{11}C, ^{13}N, and ^{15}O can be produced due to particle interactions with the dominant constituent atoms of air, ^{14}N (78.1%) and ^{16}O (21.2 %). The nuclear processes responsible for the production of these radionuclides are spallation reactions and simple "direct" nucleon transfer mechanisms. Furthermore, ^{40}Ar is sufficiently abundant (0.46 %) in the atmosphere to make possible significant production of ^{41}Ar, ^{39}Cl, and ^{38}Cl. As discussed by Butala et al. (1989), under conditions in which the beam is targeted in a concrete room the production of ^{41}Ar is believed to be due to the $^{40}Ar(n, \gamma)^{41}Ar$ thermal neutron capture reaction which has a relatively large cross section ($\approx$ 610 mb). The resultant photons, and photons from other reaction processes,

are then believed to produce ^{39}Cl and ^{38}Cl by means of (γ,p) and (γ,pn) reactions on ^{40}Ar, respectively.

Several years ago, a set of measurements of airborne radionuclides released from several target stations at Fermilab was reported by Butala et al. (1989). That paper described the general method used and the calibration practices employed at that time. It also gave a description in some detail of the target stations involved. The present work describes a new set of measurements and their calibration made at one of these target stations. This station is called the Antiproton Target Hall, which is locally known as "AP0". This facility is utilized to produce a beam of antiprotons. The antiprotons are stored in a ring of magnets and subsequently accelerated to high energies by the Tevatron accelerator and collided with a proton beam, accelerated simultaneously to the same kinetic energy (800-900 GeV). The resulting interactions form a major component of the high energy physics research program at Fermilab. During typical anti-proton production operations at AP0, a beam pulse averaging 1.6×10^{12} 120 GeV protons per pulse impinge on a target. Pulses are delivered every 2.4 sec. The target assembly consists of a stack of nickel, copper, and aluminum foils and powdered rhenium. The air emerging from this target station is continuously vented to the outdoors and the released radioactivity is measured by a flow-through ionization chamber that is used as a relatively simple stack monitor. It is the calibration of this stack monitor that forms the subject of this paper. In the next section, the apparatus will be described; and in the following section a description of actual measurements of radionuclide emissions is given after which data analysis, calibration factor determination, and discussion of the results are presented. An appendix to the paper gives the details of an absolute efficiency calculation.

EXPERIMENTAL APPARATUS

To determine the calibration factor, several different measurements were performed. These included the measurement of the flow rate of the ventilation stack by using a precision

velometer, the collection and subsequent analysis of a grab sample of the air vented using a multi-channel scaler (MCS) technique and γ-ray spectroscopy to determine the radionuclide composition of the sample, as well as the use of γ-ray spectroscopy on filters placed in the AP0 exhaust stack sampling line to determine the trace radionuclides present in emissions. An analysis using γ-ray spectroscopy of the emissions from a grab sample was conducted simultaneously with the MCS analysis. The MCS technique is needed to distinguish between the airborne positron-emitters (principally ^{11}C, ^{13}N, and ^{15}O) because their γ-ray spectra are dominated by the photons (0.511 MeV) due to the annihilation of positrons. This technique uses the life-times of the radionuclides as their signature. Gamma-ray spectroscopy can, then, be used to identify the other possible radionuclides; ^{41}Ar, ^{39}Cl, ^{38}Cl, and ^{82}Br. A schematic of the experimental setup is shown in Fig. 1. The AP0 stack is about 2.7 meters high, has an inner diameter of 25.4 cm, and has a flow rate of 0.52 m^3s^{-1}.

A fraction of the exhaust air emerging from the AP0 stack (< 0.05 %) was diverted through a sampling line inserted in its center to the grab-sample container or a filter. A metallic (copper) sampling line was used in order to eliminate absorption and adsorption due to the minimization of electrostatic pickup. In order to minimize the time required to collect a sample of the stack exhaust, a mechanical pump was connected to the output of the grab sample container through an air flow meter. This pump pulled the air through the container and flow meter to the pump exhaust. It is believed that approximate isokinetic conditions were achieved sufficient to assure the collection of a representative sample. Air in the sampling line passed through a manifold which was constructed such that the sampled gas could either pass through a filter or be routed directly to the grab sample container. Two different containers were used to contain the grab sample. The first was an ordinary sealed paint can. It was constructed of tin with a 0.025 cm thick wall, a 16.51 cm diameter, and 19.05 cm height. The second container that was used for grab-sampling consisted of a lead "pig"; that is, a right-circular cylindrical container inserted inside a 5.08 cm thick cylindrical lead shield†. Both of

these containers were fitted with inlet and outlet gas ports and a thin window 4.44 cm diameter GM tube[§].

MCS detector system

The output signal of the GM tube detector was sent to a Ludlum rate-meter[••], which provided an analog display and a standard digital output signal (TTL logic). The rate-meter was modified to generate one positive output pulse for every input pulse. The output signal was sent to the MCS module[††], which was connected to a multi-channel analyzer (MCA) equipped with an external analog to digital converter (ADC) and interfaced to a micro-computer data acquisition system[§§] (S100). For each count input to the MCS unit the MCA performs an "add one to memory" cycle at a channel representing the current dwell address. At the end of the selected dwell time the unit will advance to the next channel automatically, until the end of the selected range is reached. Thus one can collect a tabulation of the decay rate of the sample as a function of time.

HpGe detector system

A high purity Germanium (HpGe) detector[##] was used to analyze the γ-ray emissions from the paper filter, the activated charcoal filter, and the paint can as it was being counted by the multichannel scaler. The heart of this particular detector is an HpGe crystal having an active radius of 2.75 cm and an active depth of 4.29 cm. It is physically located 0.427 cm from the aluminum end cap of the detector assembly. Adding the inactive skin depth of 0.07 cm of the detector to the physical separation gives a total distance from the end cap to the active crystal face of 0.497 cm. An integral preamp is included in the detector assembly so that the output signal can be taken directly into a spectroscopy amplifier[¶¶]. The output of the spectroscopy amplifier was fed into the ADC input of a multichannel buffer[•••] which was interfaced to a microcomputer[†††]. Multichannel analyzer emulation software[§§§] was used for both the data acquisition and analysis.

MEASUREMENTS

The production of radioactivity due to interactions of 120 GeV protons with the AP0 target depends on beam parameters such as pulse rate and intensity. MCS and HpGe measurements were performed during stable anti-proton production operations in order to reduce systematic errors and take advantage of a stable background radiation level. To monitor the proton beam stability during the measurements and to obtain an average proton rate, the number of protons per pulse as measured by the accelerator's main control instrumentation was continuously recorded, as is routinely done for other operational purposes.

MCS Measurements

The MCS module was set to bin data in 4096 channels with a count time of 2 seconds per channel; thus data was obtained for a total of 2.276 hours. This time period and time resolution were found to be sufficient to distinguish the decays of the possible radionuclides encountered. First, the paint can was used to take background data for 30 minutes. Second, after purging the paint can with the air coming from the stack for 10-15 minutes, a grab sample was taken by closing the outlet and then the inlet valves. This sample was then counted with the MCS system for 8192 seconds (2.276 hours). After comparing the γ-ray background to the γ-ray spectrum taken during the MCS counting, it was concluded that, as expected, there is a "cloud" present in the general environment (i.e., the source of the "background") with approximately the same composition as the nearby stack emissions. Because of this, the data taken with the paint can was not suitable for MCS analysis. Instead, the grab sample taken with the lead pig which showed an extremely low and uniform background (approximately one count s^{-1}) was used for MCS analysis. The lead pig data, after subtracting the background, was used to determine the radionuclide composition of AP0 stack emissions.

HpGe Measurements

For these measurements, the detector system was energy calibrated using a NIST traceable mixed γ-ray source[###]. This source emitted γ-rays in the same energy region as those emitted by the radionuclides typically found in accelerator emissions. The stack exhaust was then passed through a Millipore[####] cellulose filter for an hour at a flow rate of 158 $cm^3 s\ s^{-1}$. Gamma ray spectra were recorded for background measurements, for an activated charcoal filter exposed to the air stream, and for the paint can. The background spectrum was counted for a full hour and revealed a number of accelerator-produced radionuclides with very low count rates. Radionuclides seen in this background were ^{48}Sc, ^{46}Sc, ^{56}Co, ^{60}Co, ^{24}Na, ^{137}Cs, ^{40}K, and ^{41}Ar, and naturally-occurring radionuclides from the uranium series. Only ^{38}Cl, ^{39}Cl, ^{41}Ar, and ^{82}Br were observed to be statistically different from background on the activated charcoal filter. The analysis of the paint can grab sample yielded count rates for ^{38}Cl, ^{39}Cl, and ^{41}Ar which were statistically different from background.

Flow rate measurements

The AP0 stack flow rate is needed to calculate its actual yearly release of radioactivity to the environment. The air flow rate out of the AP0 stack was measured using a precision velometer.[¶¶¶] This measurement was performed in accordance with the requirements of the U.S. Environmental Protection Agency (1989). This regulation requires that at least an eight point sampling on two perpendicular diagonals in a horizontal plane be used. Two holes were drilled in the AP0 stack and fitted with the proper connectors that were capped when not in use.

ANALYSIS OF DATA

Multi-Channel Scaler Decay Curve Fitting

It is generally assumed that the grab sample is composed of several radioactive gases produced by 3 basic processes. These processes are secondary particle (principally neutron) interactions with air, primary proton interactions with air in the"air gaps" between components that are common at high energy accelerators, and interactions of the proton beam with the target. The possible candidate radionuclides and their half-lives, taken from Browne and Firestone (1986), are given in Table 1 in order of increasing half-life.

The transit time for airborne radioactivity produced at the AP0 target to reach the AP0 exhaust stack can be estimated by dividing the volume of the AP0 target vault by the rated capacity of the ventilation fan. This yields a time of approximately 1200 seconds (20 minutes) for the air around the target to be transported to the exhaust stack. This simple-minded calculation ignores "dead spaces" and the volume occupied by the beam components. In view of the configuration involved, this omission is not likely to be significant. Because of this intrinsic delay time in the detection system and similar production cross sections, the very short-lived isotopes ^{16}N, ^{10}C, and ^{14}O will not be present to any significant degree in the emissions from the stack and can be ignored in the analysis. We are thus left with six candidate radionuclides; ^{15}O, ^{13}N, ^{11}C, ^{38}Cl, ^{39}Cl, and ^{41}Ar.

Several methods are available for deconvoluting the MCS spectrum. Manual stripping, least-square fit and Chi-squared (χ^2) fit are methods which may be appropriate. However, in a multi-parameter space there usually exist several local minima that can produce a reasonable, but not necessarily the best, fit to the data. For the present analysis the Singular Value Decomposition method of Press et al. (1989) was used initially to show that the data after background subtraction fit a sum of pure exponential decays, as expected, and that no other hidden components exist. The following equation represents the condition of a sample containing a set of radionuclides with different lifetimes:

$$A(t) = \sum_{i=1}^{n} A_i e^{-\lambda_i t}, \qquad (1)$$

where A(t) is the total activity of the grab-sample at the time t. The activity of nuclide, i, at time t = 0 is given by A_i and λ_i is its decay constant. The summation is performed over the n radionuclides present. Here n = 6, for the six radionuclides discussed above. A χ^2 fit with the steepest-gradient search was then applied to the data using this equation. Large initial values for the parameters A_i were chosen to ensure that final values would lie within the defined space. The radius of this hyper-sphere of parameter space was then reduced in small steps (for example, 0.01 counts step-size). A reduced $\chi^2 < 2$ for the fit to the data was required as a constraint. Fits to the data indicated that omission of ^{15}O from the parameter set reduced the value of χ^2 for the fit. None of the other nuclides could be omitted from the parameter set without increasing the value of χ^2 of the fit. This verifies that ^{15}O, which is produced with a cross section similar to that involved in the production of ^{11}C and ^{13}N, has decayed by approximately 10 half-lives before reaching the sampling port.

There are 4096 data points available from the MCS spectrum for fitting. Several fits with $\chi^2 > 10$ were rejected, even though they appeared to be "reasonable" in visual appearance. The rejected fits were found to correspond to widely varying and sometimes physically unreasonable radionuclide compositions. The final fit with a reduced $\chi^2 = 1.17$ was found to be stable and is displayed in Fig. 2. Alternate solutions having the slightly larger value of reduced $\chi^2 \approx 1.3$ gave a composition very close to that obtained for the chosen solution. Five radionuclides were identified as the long-lived constituents of the AP0 stack emissions. The results are displayed in Table 2. To complete the analysis, the absolute efficiency of the Geiger-Müller tube as installed in the grab sample container is needed for each of the radionuclides considered in order to convert an "apparent" activity determined from the fit to the MCS data into a true activity. This GM detector efficiency calculation and its verification by measurements performed with sealed sources in solid form were carried out in

detail and is described in Appendix A. The absolute efficiency and true activities are listed in Table 2.

HpGe Analysis of Filters

Analysis of the collected γ-ray spectra was performed using a standard built-in proprietary library to guide the peak search algorithm. This algorithm was initially used for each γ-ray spectrum to identify prominent peaks and select a region around each peak for approximating the background. For strong peaks, this method works quite well. However for peaks from radionuclides present in quantities near the instrumental detection limit, this procedure was supplemented by a subsequent manual (visual) search of the spectrum. A background-subtracted peak sum was then calculated for each peak identified by either means. The manual inspection served to assure the reasonableness of the analysis.

For the measurement of the emissions from the sampled stack ventilation stream, the gamma ray spectrum from the Millipore cellulose filter yielded a count rate for the 0.511 MeV peak that was approximately 2.5 times the average background count rate. No other radionuclides were observed on this filter. A much different spectrum was observed from analysis of the activated charcoal filter used to collect background data. As previously mentioned, ^{38}Cl, ^{39}Cl, ^{41}Ar, and ^{82}Br were all identified in the spectrum from this matrix. Although the counting geometry was not as well controlled as it would normally be in a laboratory, one can still estimate the activities of the various radionuclides on the filter since the intrinsic full peak efficiencies (ε) for the HpGe detector system are well-known from laboratory calibrations with a NIST traceable mixed γ-ray source.

The following equation was used to estimate the radionuclide specific activities, S_A, (Bq/m^3) for each excitation, corrected where necessary for the finite life time (meanlife), τ, of the radionuclide:

$$S_A = \frac{\Sigma}{\Omega_F V B_R \varepsilon A_b \tau \left\{1 \pm \exp\left(\pm L_t / \tau\right)\right\}}, \qquad (2)$$

where L_t is the live time of the count (seconds), Σ is the number of counts in the peak of interest, V is the volume of exhaust gas passed through the filter (m^3), B_R is the branching ratio for a particular gamma ray excitation, Ω_F is the average fractional solid angle (i.e., the fraction of 4π) subtended by the detector at the source, A_b is the absorption correction factor, and ε is the intrinsic full peak efficiency of the detector for the energy of the γ-ray being measured. The average solid angle, Ω_F, was estimated using the method of Gardner and Verghese (1971) for a coaxial circular disk detector and circular disk source. Multiplying the volume flow rate by the time the filter was in the sample line gave the total volume of gas which passed through the filter. The branching ratios were taken from Browne and Firestone (1986) and the efficiencies of the HpGe as a function of energy were taken from standard measurements made at Fermilab's Activation Analysis Laboratory to characterize this same detector for precision analytical work. Results of these calculations, including error analysis are presented in Table 3.

HpGe Analysis of the Paint Can γ-ray Spectrum

During the first hour of the MCS decay curve data collection for the paint can grab sample a γ-ray spectrum was simultaneously taken using the HpGe detector system. Analysis of this spectrum was performed in a manner identical to that explained above for the activated charcoal filter. Since the paint can wall is very thin and the gamma ray energies for the radionuclides of interest were generally high, the absorption correction factor was set to unity. The average solid angle subtended by the detector at the paint can source was estimated using the method of Rizk et al. (1986), for a disk detector coaxial with a right circular cylindrical source. Table 4 presents the results of these analyses.

Flow Rate of AP0 Stack

The AP0 stack flow rate was measured by inserting two sampling ports into the air flow at nine distances from the inside wall of AP0 stack along the diagonal. The opening into the sampling ports was perpendicular to the direction of air flow. The results of these

measurements are given in Table 5. The inner diameter of AP0 stack is 25.4 cm. The connector on the AP0 stack and the adapter on the precision velometer result in a 4.4 cm offset that should be added to the measured distances given in Table 5. Weather conditions for these measurements were an ambient temperature of approximately - 2 ^{o}C (271 ^{o}K) with gusting winds of approximately 40 to 50 km hr $^{-1}$ (approximately 12 m s $^{-1}$). This measurement was thus performed under rather turbulent meteorological conditions. Under such conditions it is expected that the standard deviation of the flow rates would be maximized. The average air velocity from all the above measurements was determined to be 7.62 ± 0.62 m s^{-1}. The average volume flow rate, dV/dt, is given by:

$$\frac{dV}{dt} = \text{Area} \times \text{Velocity} = \pi \left(0.127 \text{ m}\right)^2 \times [7.62 \pm 0.62 \text{ (m s}^{\pm 1})] = 0.39 \pm 0.03 \text{ m}^3 \text{ s}^{\pm 1}. \quad (3)$$

This measurement was checked against the flow rate of the building ventilation system as it was engineered. The engineered flow rate is 0.52 m^3 s^{-1}. Independent measurements of the ventilation verified that there is a leakage rate of 0.14 m^3 s^{-1} from the building aside from that from the ventilation stack monitored for radioactivity release. This leakage thus fully accounts for the difference between the engineered value for the building and the rate of release through the stack.

STACK MONITOR CALIBRATION FACTOR

The average number of protons targeted per second, dB/dt, and the stack volume flow rate dV/dt, can be used to determine the number of protons incident on the target per unit volume of air released, dB/dV,

$$\frac{dB}{dV} = \frac{dB/dt}{dV/dt} \quad . \tag{4}$$

The activity concentration, C_i, due to the i^{th} radionuclide found in the grab sample is calculated using

$$C_i = \frac{A_{si}}{V_s} \ (Bq\ m^{\pm 3}) \ , \tag{5}$$

where A_{si} is the activity of the sample due to the i^{th} radionuclide (Bq) and V_s is the grab sample volume (m^3). Then, taking the sample to be representative, the actual activity of the i^{th} radionuclide released per targeted proton, dA_i/dB is obtained from

$$\frac{dA_i}{dB} = \frac{C_i\ (Bq\ m^{\pm 3})}{dB/dV\ \ (protons\ \ m^{\pm 3})} \ \ (Bq \text{ per targeted proton}), \tag{6}$$

where it is noted that the unit of time is no longer explicit. For the present measurements, dB/dt was 5.23×10^{11} protons s^{-1}, dV/dt was measured as 0.39 $m^3\ s^{-1}$, and V_s was measured to be 3.42×10^{-3} m^3.

It is also necessary to evaluate eqn (6) for the room leakage. As a conservative estimate, it was assumed that the entire 0.14 $m^3\ s^{-1}$ of "leakage" is released at the AP0 target location at a time 1200 sec (20 minutes) before the radionuclides concentrations at the stack were determined. This time is, approximately, the time required for the air around the AP0 target to reach the AP0 stack release point. To obtain the activity in the air around the target, the measured concentration of each radionuclide released at the stack, C_i, was corrected for decay using,

$$C_{i,\,-20\ \mathrm{min}} = C_i \exp\left\{\frac{20\ \mathrm{min} \times \ln 2}{t_{1/2}(\mathrm{min})}\right\}, \qquad (7)$$

where $t_{1/2}$ is the half life of the radionuclide. $C_{i,\,-20\ \mathrm{min}}$ was used instead of C_i to calculate the activity of the i^{th} radionuclide released per proton for that component that was vented as a result of the room leakage. This approach is "conservative" in that it assumes that the activity released due to leakage does not have any time to decay at all, but is instantaneously (<< 20 minutes) released as it is produced at the target.

One can then calculate the activity of each radionuclide released per targeted proton for both the release up the stack and for that component released by means of room leakage. The results are given in Table 6 for the present measurement. They are based on the concentrations shown in Table 2. The very short-lived radionuclides neglected for the release by means of the stack are also neglected in the room leakage contribution. The total released activity of 146 nBq per proton is, approximately, a factor of three and half lower than the measurement reported by Butala et al. (1989) of 500 nBq per proton for ostensibly the same installation, the AP0 target station. Indeed, the same proton beam energy was involved in both measurements. However, extensive modifications to the enclosure ventilation system have been made in the intervening years to minimize both the release of these airborne radionuclides and the exposure to occupational workers due to this pathway. Furthermore, the present measurements rely on the absolute efficiency calculations described in this paper while the previous work was based upon the more general efficiency calculations of A. Peetermans (1972).

One could, in principle, calculate the annual release of radionuclides by simply multiplying the activity released per proton, for each radionuclide of interest, as has been described in this paper, by the targeted proton beam intensity integrated over the course of the year. However, one still needs to monitor such emissions regularly, and under some circumstances continuously, to assure compliance with the U.S. Environmental Protection

Agency Regulations (U.S. Environmental Protection Agency, 1989). It is thus prudent to correlate the results of an analysis such as is reported here with the data collected on a routine basis from a flow-through chamber equipped with a GM detector and used as a stack monitor.

At accelerators, the most accurate quantity measured is generally the total beam intensity. It has been verified through a number of years of operating the stack monitoring systems at Fermilab that the "counts" obtained from the detector used within such a stack monitor under stable operating conditions is approximately constant when normalized to the targeted beam. This constant is related to the calibration factor, C_F, which is determined as follows.

Under stable operating conditions, the monitor count rate, dM/dt (e.g., s^{-1}), will be proportional to the instantaneous aggregate concentration of radionuclides, C(t), under the reasonable assumption that the mixture of the various radionuclides is not time-dependent. Likewise, C(t) at any given time is proportional to the rate of beam targeted, dB/dt. Thus, these three quantities are proportional to each other:

$$\frac{dM}{dt} = k_1 C(t) = k_2 \frac{dB}{dt}. \qquad (8)$$

Starting from,

$$\frac{dA}{dM} \text{ (Bq per count)} = \frac{dA / dB \text{ (Bq per proton)}}{dM / dB \text{ (counts per proton)}}, \qquad (9)$$

the calibration factor, C_F, is then given by

$$C_F = \frac{dA / dM}{dV / dt} \left(\frac{\text{Bq s}}{\text{count m}^3} \right). \qquad (10)$$

For the particular detector system used at the AP0 stack monitor, dA/dM was determined to be 2.64×10^5 Bq (7.14 μCi) per count; this includes the leakage from the enclosure that does not leave through the stack. With this value, C_F is calculated to be 0.0393 Bq s m^{-3} per count

(3.82 X10^{-15} Ci hr cm^{-3} per count) for the AP0 stack. Thus, one can use C_F to determine the activity released during a given period of time of steady-state operation by simply integrating the counts from the detector and dividing by the rate of air release. After the total activity is determined, the detailed composition of the release can be obtained from the results of the analysis described in this paper.

DISCUSSION

The purpose of these measurements was to provide critical information necessary to accurately account for the release of radioactivity from a typical ventilation stack at Fermilab. The results are then to be used as input to modeling programs specified by environmental protection regulations to obtain the dose equivalent delivered by this pathway to members of the population (U. S. Environmental Protection Agency, 1989). In addition to the short-lived positron emitters commonly identified in such air releases at many accelerators, the present work was able to further quantify the less prominent radionuclides present (chlorine and argon isotopes). The HpGe analysis showed that the relative abundance of the chlorine isotopes is about an order of magnitude less than is that of the argon isotope. It also showed that ^{82}Br is present in the emissions, but at extremely low levels, approximately an order of magnitude below those of the chlorine isotopes. However, since the argon concentration was only about 1%, determination of the exact concentration of chlorine isotopes and ^{82}Br (which are approximately 0.1% and ~0.01% respectively) was not possible using the MCS data because of very low statistical precision of the data points obtained after decay periods sufficient to eliminate the competing shorter-lived radionuclides. Given this uncertainty, it is recommended that the percentage of the emitted radionuclides represented by the two chlorine isotopes be modeled in the specified computer modeling programs as if they are the longer lived argon isotope. This provides a conservative estimate of the dominant immersion dose equivalent rate in modeling calculations.

Identification of specific radionuclide activities using the HpGe detector system is performed at Fermilab whenever possible to provide supplemental information for characterization of the airborne radionuclides. As discussed above, the activated charcoal filter, the Millipore cellulose filter, and the paint can grab sample were all analyzed for gamma-emitting airborne radionuclides with the HpGe detector system. Due to attenuation of the already low intensity γ-rays in the thick lead-pig walls no attempt was made to detect them in this particular grab sample. Quantitative determinations for the concentrations in air were impossible for the two filters because the collection efficiencies were unknown. Only estimates of relative concentrations for chemically similar isotopes were feasible from measurements made with the filters. Measurements made on the paint grab sample provided the most reliable quantitative information concerning the concentrations of ^{41}Ar, ^{38}Cl, and ^{39}Cl in air released from the stack.

CONCLUSION

A systematic approach has been developed to analyze the radionuclide composition of the environmental release of airborne radionuclides from a high energy proton accelerator. The technique involves an absolute calibration of a continuous stack monitor as well as the analysis of the fractional composition of the effluent based upon fundamental principles. It is believed that the methods presented represent a sound basis for the determination of these releases that will satisfy regulatory requirements.

Acknowledgments - The assistance of Anthony Leveling and the staff of the Fermilab Accelerator Division in the conduct of these measurements is acknowledged. The authors also wish to thank Nancy Grossman and Elaine Marshall for their careful reading of this manuscript and their helpful comments.

REFERENCES

Baltakmens, T. Energy loss of beta particles on backscattering. Nuclear Instruments and Methods in Physics Research. 125: 169-170; 1975.

Browne, Edgardo; Firestone, Richard B; Shirley, Virginia S. Table of radioactive isotopes. New York, New York: John Wiley and Sons; 1986.

Butala, S. W.; Baker, S. I.; Yurista, P. M. Measurement of radioactive gaseous releases to air from target halls at a high-energy proton accelerator. Health Phys. 57: 909-916; 1989.

Gardner, R.P.; Verghese, K. Nuclear Instruments and Methods in Physics Research. 93: 163-167; 1971.

International Commission on Radiation Units and Measurements. Measurement of low-level radioactivity. ICRU Report 22 Washington, DC; 1979.

Jaffey, A. H. Solid angle subtended by a circular aperture at point and spread sources: formulae and some tables. Review of Scientific Instruments 25: 349-354; 1954.

Katz, L.; Penfold, A. S. Range-energy relations for electrons and the determination of beta-ray end -point energies by absorption. Reviews of Modern Phys. 24: 28-44; 1958.

Masket, A. V. Solid angle contour integrals, series, and tables. Review of Scientific Instruments. 28: 191-197; 1957.

Patterson, H. Wade; Thomas, Ralph H. Accelerator health physics. New York, New York: Academic Press; 1973: 518-531.

Peetermans, A. Calculations and experimental calibrations of air flow-through ionization chambers. Geneva, Switzerland: CERN; Report 72-12; July 1972 (in French).

Press, W. H; Flannery, B. P.; Teukolsky, S. A; Vettering, W. T. Numerical recipes: the art of scientific computing. New York: Cambridge University Press; 1989.

Rizk, A.; Hathout, A. M.; Hussein, A.- R. Nuclear Instruments and Methods in Physics Research, A245; 162-166; 1986.

Robinson, C. V. (1967). Geiger-Müller and proportional counters in Page 57 in Instrumentation in Nuclear Medicine; Hine, G. J., ed. New York: Academic Press; 1967: 57.

Seelmann-Eggebert, W; Pfenning, G.; Münzel, H; Klewe-Nebenious, H. Chart of the nuclides. Karlsruhe, Germany: Kernforschungszentrum; 1981.

Seliger, H. H. Back-scattering of positrons and electrons in Electron Physics, NBS circular 527, 3-17-54. Washington, DC: National Bureau of Standards; 1954.

Snell, A. H. (ed.). Nuclear Instruments and Their Uses, Vol. 1. New York: John Wiley and Sons; 1962: 317.

Swanson, W. P.; Thomas, R. H. Dosimetry for radiological protection at high energy particle accelerators", Chapter 1 in *The Dosimetry of Ionizing Radiation,* Volume III. New York: Academic Press; 1990: 85-88.

Tabata, T; Ito, R.; Okabe, S. An empirical equation for the backscattering coefficient of electrons. Nuclear Instruments and Methods in Physics Research. 94: 509-513; 1971.

Thomas, R. H.; Stevenson, G. R. Radiological safety aspects of the operation of proton accelerators". Vienna: International Atomic Energy Agency Technical Report No. 283; 1988: 430-440.

U. S. Environmental Protection Agency. Code of federal regulations. Washington, DC: U. S. Government Printing Office; 40 CFR Part 61 Subpart H, 1989.

Tsoulfanidis, N. Measurements and detection of radiation. Washington, DC: Hemisphere Publishing Corporation; 1983: 133-134.

APPENDIX A

β-PARTICLE EFFICIENCY CALCULATION FOR AIRBORNE GRAB SAMPLING TECHNIQUE

The amount of activated air released from the target areas at Fermilab (including the station at AP0) is typically quantified using a thin 4.44 cm diameter end-window Geiger-Müller (GM) tube installed inside a thick-walled lead canister† as shown in Fig. A1. This arrangement is used to take a grab sample of the activity as described in this paper. As discussed in this paper, several different radionuclides are found in a typical grab-sample taken from the AP0 stack. These radionuclides emit different combinations of positrons, electrons and gamma-rays. To convert the "raw" count rate from a GM tube to a measurement of activity, the absolute detection efficiency, ε, of the tube is required. This Appendix describes the method used to calculate this efficiency.

In general, the detection efficiency of GM tubes depend on the energy and type of incident radiation. Gas-filled detectors generally have reasonably good intrinsic efficiency ($\varepsilon \approx 1$) for charged particles, such as β-particles emitted by the radionuclides of concern, but have much poorer efficiency for photons such as the γ-rays emitted by these radionuclides. The intrinsic absolute efficiency of GM tubes to γ-rays is less than 0.01 and is a slowly decreasing function of photon energy. Thus, the results of a measurement of the activity within the sampling volume of the container can be regarded as being solely based upon the β-particle detection efficiency. A calculation of the parameters used to determine the β-particle detection efficiency of GM tubes§ used in our measurements is described.

The GM tube's detection efficiency was calculated using

$$\varepsilon_{GM} = f_{geom}\, f_{dt}\, f_{bksct}\, f_{\beta}\, f_{self \pm abs}\, f_{trans}\ . \qquad \text{(A1)}$$

The factors in the above equation will be described in the following sub-sections and the method of calculation employed for each one will be presented. Comparisons will be made with calculations based upon this same technique for sealed sources comprised of radionuclides which emit β-particles of similar energy. Finally, the value of ε_{GM} for the airborne radionuclides of concern in the present work are presented.

Geometry Factor f_{geom}

The geometry factor is defined as the fraction of the total solid angle subtended by a source to a detector aperture. The solid angle presented by an extended cylindrical source to a circular aperture detector was approximated by calculating the solid angle presented by a disk source and a circular aperture detector, as shown in Fig. A2, having the same diameter as the GM tube used in the study. The method described by Jaffey (1954) and Masket (1957) was employed and results in

$$f_{geom} = G_p \left\{ 1 \pm \frac{3}{8} b^2 \left[\frac{H\,(H + D)}{D^4} \right] \right\}, \qquad \text{(A2)}$$

where b is the radius of the source, H is the distance between the source and detector and D is given by

$$D = \sqrt{H^2 + a^2}\ , \qquad \text{(A3)}$$

where a is the radius of the detector aperture. G_p is the fractional solid angle for a point source on the axis of a circular aperture detector given by

$$G_p = \frac{1}{2} \left[\frac{a^2}{D(D + H)} \right]. \qquad \text{(A4)}$$

Dead time correction f_{dt}

The GM tube and its associated electronics form a nonparalyzable system with a characteristic pulse resolving time, or dead time, that is related to the time required to process individual detected events. This dead time causes the loss of detected events, but it can be corrected for if the pulse width and the detected count rate are known, using

$$R_{true} = \frac{R_d}{1 - R_d\tau}, \qquad \text{(A5)}$$

where R_{true} is the "true" count rate, R_d is the detected count rate and τ is the resolving time. In the present situation, the output signal pulse of the GM tube, after processing, had a maximum width of 70 microseconds. The ratio R_d/R_{true} is then used as f_{dt}. For the air sample measurements described here, f_{dt} was calculated to be 0.9978.

Back-scattering f_{bksct}

Large-angle deflection of β-particles along their track is the phenomenon of back-scattering. The amount of back-scattering is dependent on the atomic number, thickness of the scatterer, and the beta-particle energy as has been stated by Tabata et al. (1971). Back-scattering of β-particles from the sample and its container increases the sample counting rate and can amount to 10-40 percent of the total counting rate. Following Tabata et al. (1971) the back-scattering fraction is calculated using

$$\eta = \frac{a_1}{1 + a_2\tau^{a_3}}, \qquad \text{(A6)}$$

where τ is the average kinetic energy of the β-particle in units of electron rest energy (0.511 MeV) and the a_i are target-dependent parametrizations given by

$$a_1 = b_1 \exp\left(-b_2 Z^{-b_3}\right),$$
$$a_2 = b_4 + b_5 Z^{-b_6}, \qquad \text{(A7)}$$
$$a_3 = b_7 - \frac{b_8}{Z}.$$

The constants b_i were obtained by Tabata et al. (1971) from fits to a large set of experimental data ranging from about 50 keV up to 22 MeV in energy and atomic number, Z, from 6 to 92:

$$b_1 = 1.15 \pm 0.06 \qquad b_2 = 8.35 \pm 0.25$$
$$b_3 = 0.525 \pm 0.020 \qquad b_4 = 0.0185 \pm 0.0019$$
$$b_5 = 15.7 \pm 3.1 \qquad b_6 = 1.59 \pm 0.07 \quad . \qquad \text{(A8)}$$
$$b_7 = 1.56 \pm 0.02 \qquad b_8 = 4.42 \pm 0.18$$

The back-scattering coefficient is

$$f_{bksct} = 1 + \eta \quad . \qquad \text{(A9)}$$

The energy of the back-scattered β-particle depends on the incident energy and the scattering angle. Because of the continuous energy spectrum of the beta-particles, the two quantities commonly used are the maximum and the average β-decay energies (Browne and Firestone 1986). For the back-scattering approximation one also has to sum and average over the backward angles. Due to the complexity of the analytical calculations involved, an empirical relationship found by Baltakmens (1975) was used. This relation is obtained by fitting to a range of β-emitting nuclides of atomic numbers from 10 to 92 and β-energies from 100 keV to 4 MeV:

$$\frac{E_s}{E_m} = \frac{158 + Z}{251}, \qquad \text{(A10)}$$

$$\frac{\bar{E}_s}{\bar{E}} = \frac{123+Z}{216}, \qquad \text{(A11)}$$

where E_s and $\bar{E}_s$ are the energies of the back-scattered β−particle of maximum energy E_m and average energy $\bar{E}$, respectively. The container used to determine the radionuclides in a grab sample of the emissions from the AP0 stack is contained inside of a lead container (Z = 82). Forty percent of the β-particles back-scatter from the lead walls and lose only 5 % of their kinetic energy.

Back-scattering of positrons versus electrons, $f_{\beta^\pm}$

Based only on single scattering cross section, there is an excess of electrons back scattered compared to positrons back-scattered. Experimental results of Seliger (1954) show a relatively weak Z dependence and an average value of $\beta^-/\beta^+ = 1.3$. The theoretically calculated value is lower than experimental measurements (1.1 for Z = 80). Considering these factors and their uncertainty, a value of 1.2 was adopted in this paper. The back-scattering calculations presented in the previous subsection ignores this effect; therefore, it is included here as a separate factor.

Self- absorption f_{slf_abs}

A sample can absorb some of the beta-particles it emits, as has been described by Snell (1962) and Robinson (1967), and as reviewed by the ICRU (1979). This phenomenon of self-absorption depends on the sample thickness and the β-particle energy. Self-absorption will affect the observed counting rate of the sample. It is assumed that beta-particles undergo approximate exponential attenuation, with a half thickness h(E) that is a function of β-particle energy. The counting efficiency depends on source thickness, t, (assuming the source diameter remains constant) and the absorption efficiency, ε_{abs}, is given by

$$\varepsilon_{abs} = \frac{h(E)}{0.693\ t}\left[1 - \exp\left(\frac{-0.693\ t}{h(E)}\right)\right]. \qquad \text{(A12)}$$

It is assumed that h(E), the half value layer in mg/cm^2 is given by $h \approx 0.1\ R_o(E)$, where $R_o(E)$ is the range of the β-particle. Trajectories of electrons through matter are not straight. Electrons go through large deflections due to their collisions with atomic electrons. As the energy of the electron traversing material increases, energy loss due to radiation increases exponentially. Electrons do not have a well-defined range as do heavy charged particles. Based on empirical data of Katz and Penfold (1958), the following relation for the calculation of the ranges of β-particles has been obtained. This relation is valid for electrons of 10 keV up to 3 MeV kinetic energy, which is more than sufficient for the β-particles of concern in the present work:

$$\begin{aligned} R_o &= 412\ E^n\ \left(\text{mg/ cm}^2\right) \\ n &= 1.265 - 0.0954 \times \ln(E) \end{aligned}\ , \qquad \text{(A13)}$$

where E is the β-particle kinetic energy in MeV. The transmission efficiency is then calculated using

$$F_{slf\_abs}(E) = 1 - \varepsilon_{abs}\ , \qquad \text{(A14)}$$

The value of f_{slf_abs} to be used in eqn (A1) can be obtained by performing a weighted average over the self-absorption of the direct β-particles and those that are back-scattered with the energy $\bar{E}_S$ [see eqn (A11)],

$$f_{slf\_abs} = \frac{F_{slf\_abs}(E) + \eta\ F_{slf\_abs}\left(\bar{E}_S\right)}{f_{bksct}}\ . \qquad \text{(A15)}$$

Window transmission f_{trans}

The fraction of beta-particles transmitted through the GM tube's thin window depends mainly on the thickness of the window and the beta-particle incident energy. The transmission of both direct and the scattered betas through the GM tube's thin window was calculated as follows. The fraction of betas transmitted through a thickness, t, has been experimentally observed to be represented by:

$$T = e^{-\mu t}, \qquad \text{(A16)}$$

where μ is the mass absorption coefficient. The value of the μ has been determined to be well-described as a function of maximum beta energy by Tsoulfanidis (1983),

$$\mu = 0.017 \; E_{max}^{-1.14} \; \left(cm^2 \; mg^{\pm 1}\right) \qquad \text{(A17)}$$

where E_{max} is in MeV. The thickness t used in eqn (A16) is expressed in units of mg cm^{-2}. The transmission factor was obtained for the direct β-particles and for the fraction that was back-scattered with the energy $\bar{E}_S$. A weighted average of the direct and back-scattered transmission factors was used to obtain f_{trans}, the quantity to be used in eqn (A1),

$$f_{trans} = \frac{T_{direct} + \eta T_{backscattered}}{f_{bksct}} \quad . \qquad \text{(A18)}$$

Check of Method of Efficiency Calculations

In order to corroborate the results of calculations using this set of equations, the efficiency of the GM tube, given by eqn (A1), present in the container used for the airborne grab sampling was calculated for several β-emitting standard sealed sources whose strengths were well-understood because of previous direct efficiency measurements needed for the

calibration of an automatic planchet counting (APC) system used to count wipe samples at Fermilab¶. The sources were placed on blank planchets with aluminum backing having the same diameter as the GM tube, which is 4.45 cm (1.75 inches). The source to detector separation was 1.0 ± 0.1 cm. Self-absorption in the source material was ignored, since the sources used were extremely thin. However, back-scattering is not negligible and the results using the method described above are that ten percent of the β-particles back-scatter from the aluminum backing of the sample-changer's calibration sources and, as discussed above, lose about 37% of their energy upon back scattering. The calculated and measured efficiencies for these solid sources are given in Table A1. The agreement is quite good and verifies major elements of the technique and some of the factors in eqn (A1). However, this measurement does not provide a complete check of all factors of this equation as encountered with an air sample. For the remainder, one must rely on the validity of the theoretical calculations of the various quantities.

Results of Calculations of Detection Efficiency of the GM Tube

The GM detector used for the AP0 measurements had a 4.45 cm (1.75 inch) diameter mica window with an average thickness of 1.7 mg/cm^2. The lead-pig used for taking samples of airborne radionuclides has a right circular cylinder dimensions of 13.81 cm diameter and 22.9 cm height. Since the distance between the air sample and the GM detector is not fixed as it would be for a point source of solid material, but instead ranges over the entire volume of the chamber, a mean value for f_{geom} was estimated by averaging over an assumed one thousand distances ranging from zero to 22 cm, for source-to-detector separation. This average value was determined in this manner to be $f_{geom} = 0.131$.

The maximum count rate in actual measurements of airborne radionuclides was about 35 counts per second and this value was used for dead time corrections. The calculated parameters and efficiencies for the radionuclides expected to be of concern in the emissions from AP0 are presented in Table A2. The values of ε_{GM} are carried over into Table 2 as well.

List of Figure Captions

Figure 1 Schematic drawing of experimental arrangement for AP0 stack emissions measurements.

Figure 2 Chi-square fit to the background subtracted MCS data taken with the lead pig. Data are in two second bins, and for clarity only 5% of the 4096 data points are shown.

Figure A1 Schematic drawing of stack monitor used at AP0. The walls are 5.08 cm thick lead. The inside radius of the circular cross section is 6.9 cm and the depth of the cylinder is 22.9 cm.

Figure A2 Relation of source and aperture for efficiency calculation. The upper circle is representative of a circular aperture of a detector while the lower circle represents a parallel disk source centered on the counter axis. The relevant parameters H, D, a, and b are described in the text.

List of Table Captions

Table 1. Gaseous isotopes produced from beam-air interactions. Half-lives are given in seconds (s) and minutes (m).

Table 2. Radionuclide composition of the AP0 grab-sample determined from MCS technique. In this table A_o is the initial activity determined each component, $\%A_o$ is the percentage of the total activity for each component, ε_{GM} is the detector efficiency for the Geiger-Mueller tube, A_{true}, is the true activity of each radionuclide corrected for the detector efficiency, and $\%A_{true}$ is the percentage of the total activity of each component corrected for detector efficiency.

Table 3 Specific activities of radionuclides measured using HpGe analysis of the activated charcoal filter after 3 hours in the AP0 exhaust stack sampling line. The errors are weighted over the results for the available excitations.

Table 4 Specific activities of radionuclides measured using HpGe analysis of the paint can sample. The errors are weighted over the results for the available excitations.

Table 5. Measurements of the AP0 stack flow rate. Distances are in centimeters and air speeds for ports 1 and 2 are in meters per second.

Table 6 Activity per proton at each of the release points due to the various radionuclides. Activities are given as nBq/target proton.

Table A1 Comparison of the measured and calculated efficiencies for β-emitting sources used for APC system calibration.

Table A2 Calculated parameters and efficiencies for the common β-emitting isotopes identified in airborne emissions at Fermilab for the stack monitor instrumentation used at AP0.

Nuclide	^{16}N	^{10}C	^{14}O	^{15}O	^{13}N	^{11}C	^{38}Cl	^{39}Cl	^{41}Ar
Half-life	7 s	19 s	1.18 m	2.04 m	9.97 m	20.39 m	37.24 m	56.60 m	109.6 m

Table 1

Nuclide	^{11}C	^{13}N	^{38}Cl	^{39}Cl	^{41}Ar
A_o	33.8	27.0	1.1	1.1	1.1
$\%A_o$	52.7	42.1	1.7	1.7	1.7
ε_{GM}	8.5%	10.4%	16.3%	14.2%	10.5%
A_{true} (Bq)	199.9	130.4	3.4	3.9	5.2
$\%A_{true}$	58.3	38.0	1.0	1.1	1.5

Table 2

Nuclide	Gamma Excitation Energy (keV)	Estimated Specific Activity (Bq m^{-3})	Error in Specific Activity (Bq m^{-3})	Weighted Average (Bq m^{-3})	Weighted Error (Bq/m^{-3})
^{38}Cl	1642.4	21.6	2.5		
	2167.5	21.3	1.9	21.5	1.2
^{39}Cl	250.3	18.9	2.1		
	1267.2	17.2	1.6		
	1517.4	20.2	2.0	18.4	1.1
^{41}Ar	1293.6	11.4	0.9	11.4	0.90
^{82}Br	554.3	1.34	0.44		
	776.5	1.49	0.41	1.42	0.30

Table 3

Nuclide	Gamma Excitation Energy (keV)	Estimated Specific Activity (Bq m^{-3} X 10^4)	Error in Specific Activity (Bq m^{-3} X 10^4)	Weighted Average (Bq m^{-3} X 10^4)	Weighted Error (Bq m^{-3} X 10^4)
^{38}Cl	1642.4	1.00	0.42		
	2167.5	1.20	0.20	1.17	0.18
^{39}Cl	250.3	0.819	0.530		
	1267.2	0.895	0.292		
	1517.4	0.879	0.304	0.878	0.194
^{41}Ar	1293.6	8.05	0.35	8.05	0.35

Table 4

Position No.	1	2	3	4	5	6	7	8	9
Distance (cm)	0.81	2.67	4.93	8.2	12.7	17.2	20.47	22.73	24.59
Port 1 (m/s)	7.62	6.10	6.86	7.11	7.62	7.62	9.65	9.65	8.13
Port 2 (m/s)	8.13	6.60	6.86	7.11	7.62	7.62	7.62	7.62	7.62
Average (m/s)	7.87	6.35	6.86	7.11	7.62	7.62	8.64	8.64	7.87

Table 5

Nuclide	Stack (nBq/proton)	Leakage (nBq/proton)
^{13}N	27.49	41.43
^{11}C	42.16	31.21
^{38}Cl	0.71	0.39
^{39}Cl	0.82	0.39
^{41}Ar	1.11	0.47
Total (nBq/proton)	72.28	73.89
Total Released (nBq/proton)		146.2

Table 6

Nuclide	$\bar{E}_{\beta}(MeV)$	$\beta\pm$	$\varepsilon_{calculated}(\%)$	$\varepsilon_{measured}(\%)$
^{14}C	0.04947	β^-	3.7 ± 0.2	3.8 ± 3.4
^{22}Na	0.21554	β^+	15.7± 2.	14.9 ± 3.3
^{90}Sr (^{90}Y)	0.1958 (0.9348)	β^-	42.0± 2.5	40.5 ± 2.4
^{99}Tc	0.08460	β^-	9.9± 0.5	9.2 ± 3.2

Table A1

Nuclide	$\bar{E}_\beta$ (MeV)	$f_{\beta^\pm}$	f_{bksct}	$f_{self\text{-}abs}$	f_{trans} (%)	ε (%)
^{13}N	0.4918	β+	1.413	0.599	0.936	10.4
^{11}C	0.3856	β+	1.417	0.498	0.916	8.5
^{38}Cl	1.553	β-	1.435	0.882	0.982	16.3
^{39}Cl	0.821	β-	1.479	0.763	0.964	14.2
^{41}Ar	0.464	β-	1.497	0.575	0.932	10.5

Table A2

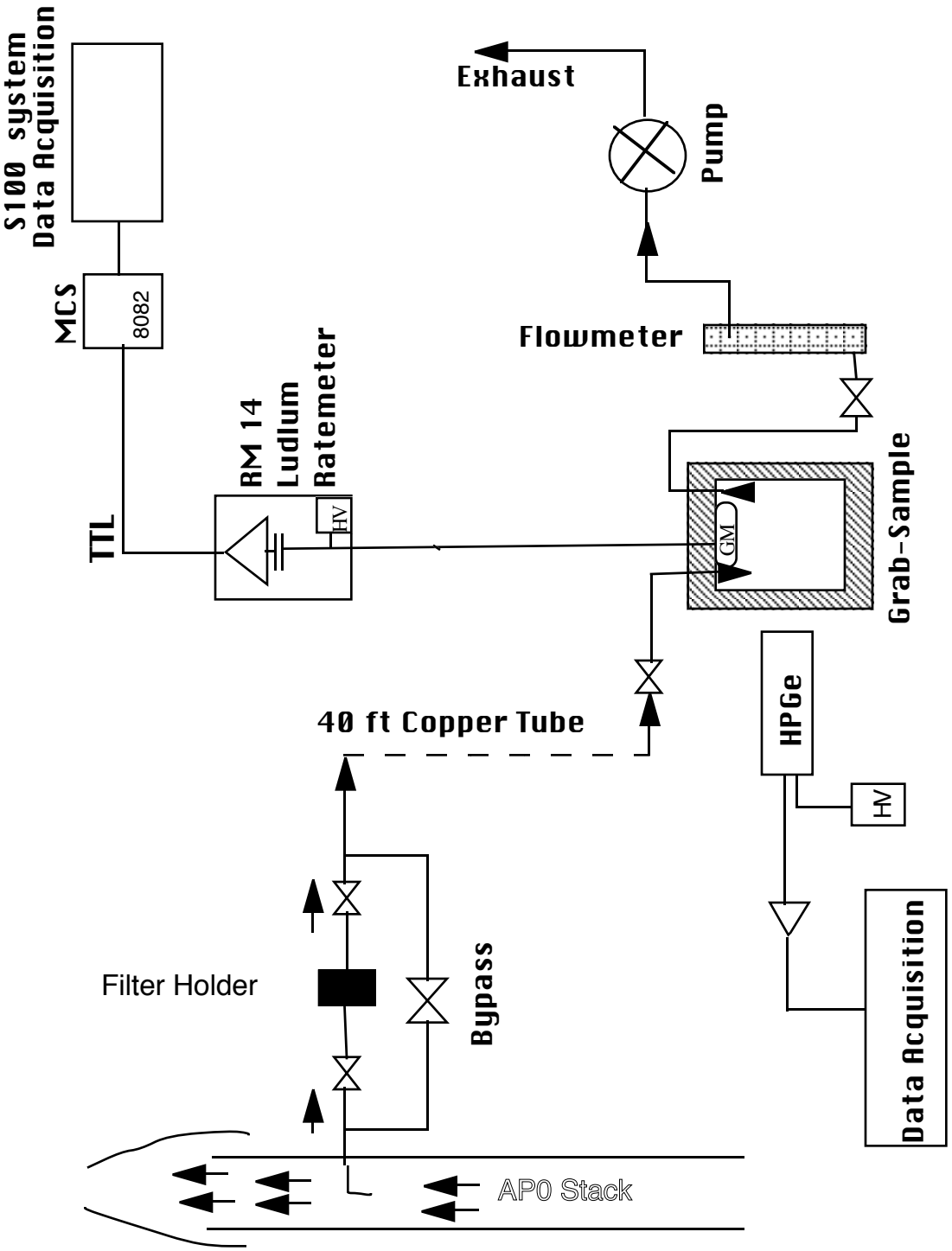
S100 system
Data Acquisition
MCS
8082
TTL
RM 14
Ludlum
Ratemeter
HV
Exhaust
Pump
Flowmeter
GM
Grab-Sample
HPGe
HV
40 ft Copper Tube
Filter Holder
Bypass
Data Acquisition
AP0 Stack

Figure 1

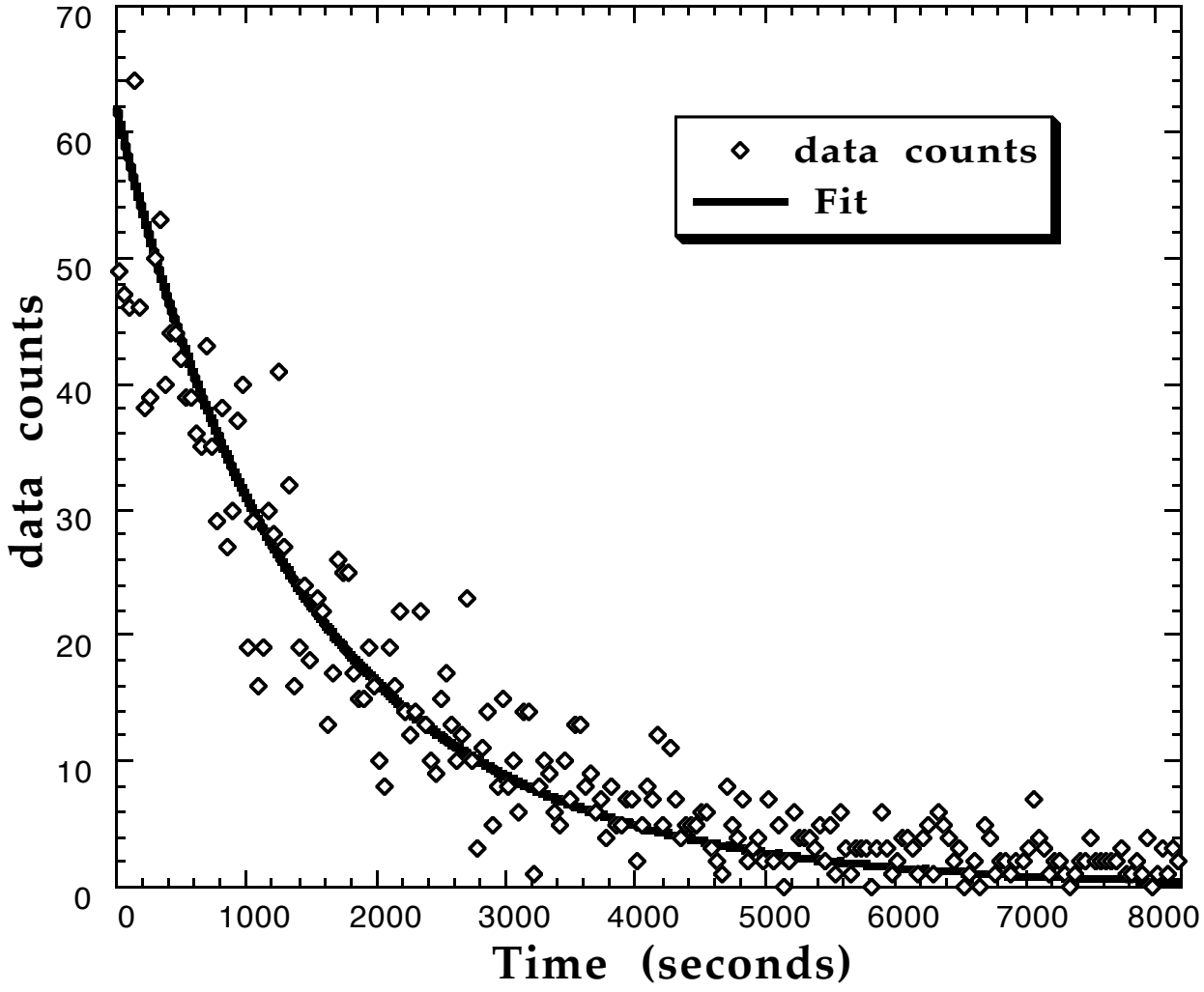
data counts
Fit
data counts
Time (seconds)
0
10
20
30
40
50
60
70
0
1000
2000
3000
4000
5000
6000
7000
8000

Figure 2

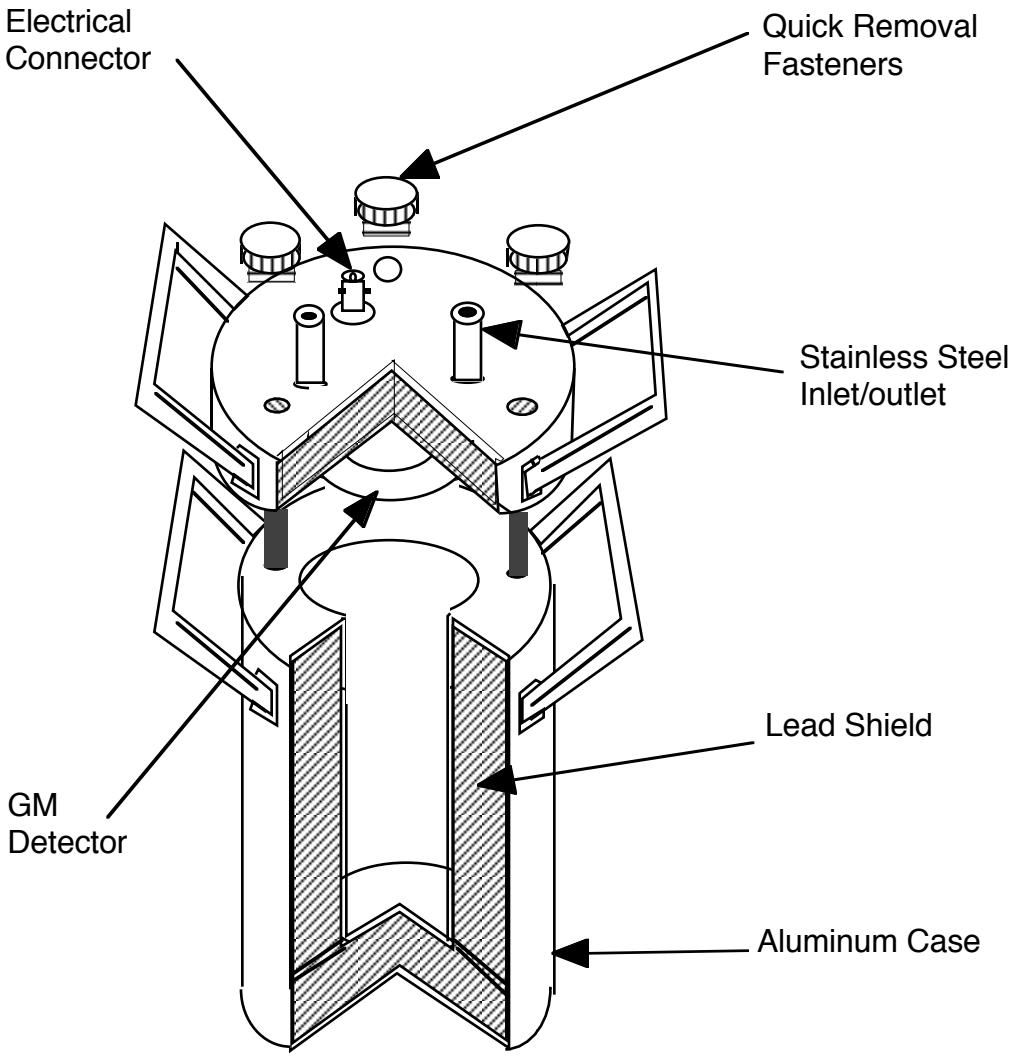
Electrical
Connector
Quick Removal
Fasteners
Stainless Steel
Inlet/outlet
Lead Shield
GM
Detector
Aluminum Case

Figure A1

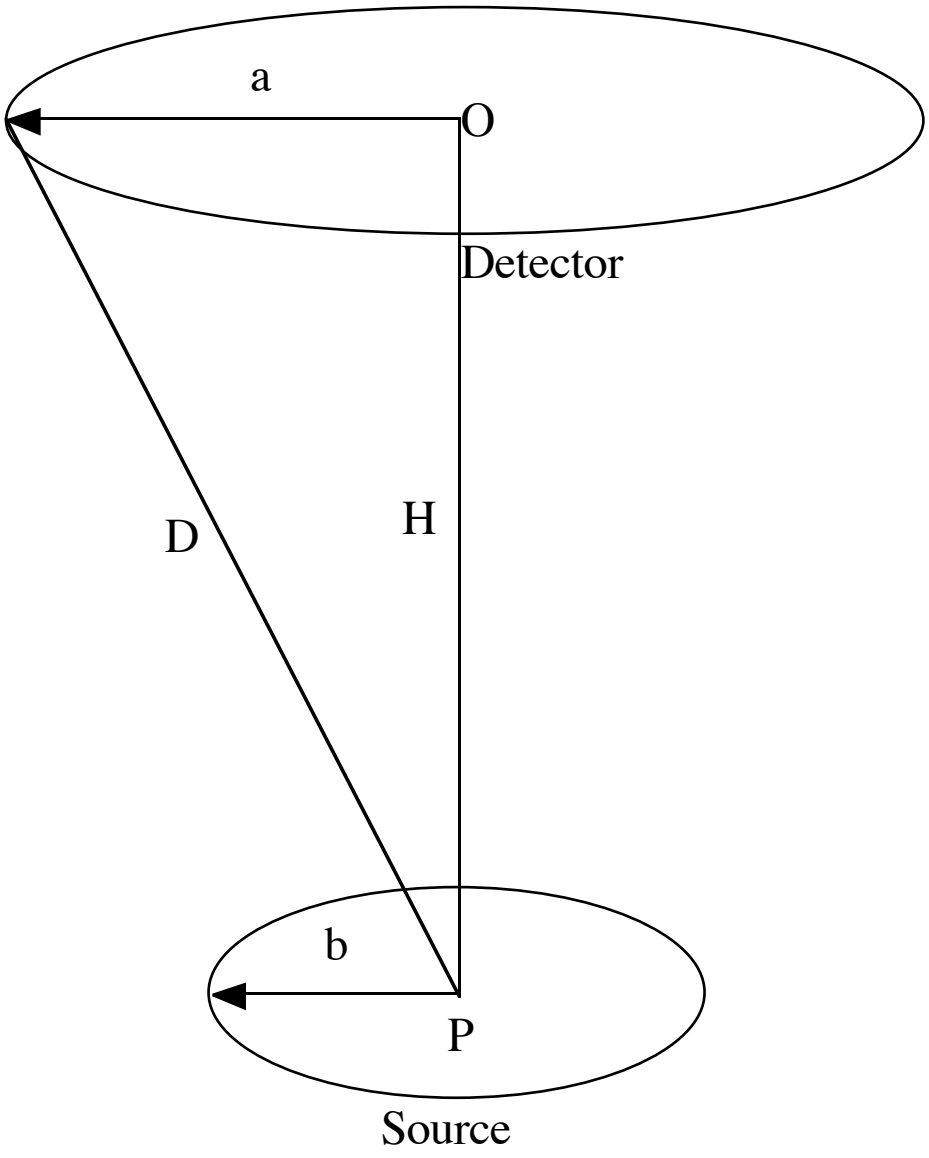

Figure A2

This work was performed at the Fermi National Accelerator Laboratory, which is operated by Universities Research Association, Inc., under contract DE-AC02-76CH03000 with the U. S. Department of Energy.

•• Ludlum, rate-meter, 177-4. Ludlum Measurements Inc. P. O. Box 810, 501 Oak, Sweetwater, Texas 79556.

†† MCS UNIT, Model 8082, Operator's Manual, Canberra Industries, Inc., One State Street, Meriden, CT 06450.

§§ System S100, Hardware and Software, Canberra Industries, Inc., One State Street, Meriden, CT 06450.

GEM Series high purity Germanium (HpGe) detector, Serial # 28-TP30036B, EG&G ORTEC, 100 Midland Road, Oak Ridge, TN., 37831-0895.

¶¶ Model 671 Spectroscopy Amlifier, EG&G ORTEC, 100 Midland Road, Oak Ridge, TN., 37831-0895.

••• Model 918A Multichannel buffer, EG&G ORTEC, 100 Midland Road, Oak Ridge, TN., 37831-0895.

††† BSI-V Portable 486-33 ISA computer, 918A, EG&G ORTEC, 100 Midland Road, Oak Ridge, TN., 37831-0895.

§§§ MAESTRO II MCA Emulation Software, EG&G ORTEC, 100 Midland Road, Oak Ridge, TN, 37831-0895.

Mixed radionuclide γ-ray reference standard, Model QCD.1, Amersham Corporation, 2636 Clearbrook Drive, Arlington Heights, Illinois.

####NATLSCO - A KRMS Company, 1 Kemper Drive K-2, Long Grove, IL 60049-0075.

¶¶¶ Kurz Velometer Model 441, S. Kurz Instruments Inc. 2411 Garden Rd. Monterey, CA 93940.

†Counting Chamber Stack Monitor Model CG-11X2, Tchnical Associates, 7051 Eton Avenue, Canoga Park, CA 91303.

§ Model N1002/8767, TGM Detectors, Inc. 166 Bear Hill Rd., Waltham, Mass. 02154.

¶ F. Krueger, private communication documented in an internal document, Fermilab Radiation Physics Note 96 (1992).